HHS Public Access

Author manuscript

Exp Cell Res. Author manuscript; available in PMC 2020 June 12.

Published in final edited form as:

Exp Cell Res. 2018 October 01; 371(1): 20–30. doi:10.1016/j.yexcr.2018.05.028.

Heterogeneity of adult masseter muscle satellite cells with cardiomyocyte differentiation potential

Wei Huang[1,*], **Jialiang Liang**[1,*], **Yuliang Feng**[1,*], **Zhanfeng Jia**[2], **Lin Jiang**[1], **Wenfeng Cai**[1], **Christian Paul**[1], **Jianguo G. Gu**[2], **Peter J. Stambrook**[3], **Ronald W. Millard**[4], **Xiao-Lan Zhu**[5], **Ping Zhu**[5], **Yigang Wang**[1]

[1]Department of Pathology and Laboratory Medicine, University of Cincinnati College of Medicine, Cincinnati, OH, USA.

[2]Department of Anesthesiology, University of Cincinnati College of Medicine, Cincinnati, OH, USA.

[3]Department of Molecular Genetics, Biochemistry, and Microbiology, University of Cincinnati College of Medicine, Cincinnati, OH, USA.

[4]Pharmacology and Cell Biophysics, University of Cincinnati College of Medicine, Cincinnati, OH, USA.

[5]Department of Cardiac Surgery, Guangdong Cardiovascular Institute, Guangdong General Hospital, Guangdong Academy of Medical Sciences, Guangzhou, China.

Abstract

Although resident cardiac stem cells have been reported, regeneration of functional cardiomyocytes (CMs) remains a challenge. The present study identifies an alternative progenitor source for CM regeneration without the need for genetic manipulation or invasive heart biopsy procedures. Unlike limb skeletal muscles, masseter muscles (MM) in the mouse head are developed from Nkx2-5 mesodermal progenitors. Adult masseter muscle satellite cells (MMSCs) display heterogeneity in developmental origin and cell phenotypes. The heterogeneous MMSCs that can be characterized by cell sorting based on stem cell antigen-1 (Sca1) show different lineage potential. While cardiogenic potential is preserved in $Sca1^+$ MMSCs as shown by expression of cardiac progenitor genes (including Nkx2-5), skeletal myogenic capacity is maintained in $Sca1^-$ MMSCs with Pax7 expression. $Sca1^+$ MMSC-derived beating cells express cardiac genes and exhibit CM-like morphology. Electrophysiological properties of MMSC-derived CMs are demonstrated by calcium transients and action potentials. These findings show that MMSCs could serve as a novel cell source for cardiomyocyte replacement.

Corresponding authors: Yigang Wang, M.D., Ph.D., Department of Pathology and Laboratory Medicine, University of Cincinnati, 231 Albert Sabin Way, Cincinnati, OH 45267-0529 USA, Tel: (513) 558-5798, Fax: (513) 558-2141, yi-gang.wang@uc.edu; Ping Zhu, M.D., Ph.D., Department of Cardiovascular Surgery, Guangdong Cardiovascular Institute, Guangdong General Hospital, Guangdong Academy of Medical Sciences, Guangzhou, China 510080., Tel.: + 86 20 83827812-10288, Fax: + 86 20 83875453, tanganqier@163.com.

*These authors contributed equally to this work

Author Contributions

W.H., J.L., and Y.F.: conception and design, collection and assembly of data, data analysis, and writing; J.Z., L.J., W.C., and X.L.Z.: collection and assembly of data; C.P., J.G.G.: discussion and writing; P.Z. and Y.W.: conception and design, data analysis and interpretation, and financial support.

1. Introduction

Cardiac stem cell (CSC) therapy has been developed as a promising strategy to repair damaged myocardium [1, 2]. Several putative CSCs have been isolated from adult rodent or human hearts, whereas their contribution to the regeneration of cardiomyocytes (CMs) remains controversial [3-5]. The widespread use of autologous CSCs in a clinical setting has been hampered by the invasive nature of biopsy procedures and limited potential for self-renewal and cardiogenesis [6-8]. There is also controversy regarding whether mesenchymal stem cells or skeletal myoblasts can be efficaciously transdifferentiated into CMs [9, 10]. Whether authentic cardiac regeneration can be achieved from extra-cardiac cell sources remains to be addressed as a potential therapeutic option [11].

Studies of embryonic development have stimulated great interest in new source of stem cells with cardiogenic potential. The heart is formed from bilateral heart fields during gastrulation process [12]. The first differentiated myocardial cells in the cardiac crescent of the lateral splanchnic mesoderm are referred to as the first heart field (FHF) [13]. The second heart field (SHF) migrates from the pharyngeal mesoderm (PM) and lies medially and posteriorly to the crescent/FHF [14, 15]. As the embryo grows, PM also develops into cranial head muscles in close apposition to the developing heart [16-18]. Mouse and chick embryo studies have demonstrated an overlapping pattern in the expression of cranial skeletal muscle and cardiac lineage markers [19-21]. These studies demonstrate that the progenitors in the PM enact as a common ancestry for the development of head and heart muscles. The asymmetric or symmetric self-renewal of craniofacial-cardiac progenitors may result in formation of satellite stem cell pools that are maintained in adulthood [22, 23]. Satellite cells normally reside in muscle tissues with a quiescent state and intermittently replenish the stem cell pool to regenerate neighboring myofibers [24, 25]. However, the stem cell pool within the head muscles has not been systematically characterized.

In the present study, we isolated the satellite stem cells of the branchiomeric muscles derived from craniofacial-cardiac PM and identified the cell phenotypes. We demonstrate that a subpopulation of masseter muscle satellite cells (MMSCs) derived from Nkx2-5 mesoderm in adult mice is capable of differentiation into functional CMs. Proof-of-concept is provided demonstrating that CMs can be transdifferentiated from masseter muscle-derived cells. This finding provides a new progenitor cell source for CM regeneration and it offers a great potential in subsequent applications.

2. Materials and methods

All research protocols were performed under the Guidelines for the Care and Use of Laboratory Animals published by the National Institutes of Health (National Academies Press, eighth edition 2011). All animal use protocols and methods of euthanasia in this study were approved by the University of Cincinnati Animal Care and Use Committee. An independent review and approval of cell culture methods used in this study was conducted by the Institutional Biosafety Committee. Additional Materials and Methods are described in Supplemental Information.

2.1 Transgenic mice

Transgenic mice including Nkx2-5-Cre (Stock No: 024637), Rosa-RFP (Stock No: 007914), Myh6-Cre (Stock No: 011038), and Rosa-RFP-GFP (Stock No: 007576) were purchased from The Jackson Laboratory. The genotypes of these mice were authenticated using standard PCR protocols available from the Jackson Laboratory.

2.2 Isolation and culture of muscle satellite cells

Cells were isolated according to a modified myosphere protocol. Masseter or limb muscle tissue of mice (6-8 weeks old) was removed, washed, and minced. The muscles were enzymatically dissociated at 37°C for 2 hours in 0.1% collagenase II/DMEM. The tissue slurry was then dissociated with 0.125% Trypsin for 45 mins. After cell digestion, 10% FBS was added to inactivate collagenase/trypsin. The slurry was passed through a 70μm cell strainer and centrifuged for 5 mins. at 2000 rpm. Cell pellets were washed in phosphate buffer saline (PBS) and re-suspended in 10mL growth medium (containing 0.1mM nonessential amino acids, 0.1mM β-mercaptoethanol, 1000IU/mL leukemia inhibitory factor, 10ng/mL BMP-4, and 10% FBS in high-glucose DMEM). The cell suspension was filtered through a 40μm cell strainer and plated on low attachment plates for suspension culture. Growth medium was refreshed every 2 days. On day-3, the isolated cells adhered to the plates (plating) due to asymmetric cell division. The adherent cells were dissociated by using Cell Dissociation Solution (Sigma) and collected by centrifugation. The cell pellets were re-suspended with growth medium (Figure S1B) and seeded in the low attachment plates for suspension culture (re-sphere). Additionally, the microspheres of MMSCs greater than 100μm in the cell supernatant were passaged through dissociation with Cell Dissociation Solution and then centrifuged and re-suspended on the low attachment plates with growth medium. This re-sphere passaging strategy allowed for expansion of MMSCs, and isolation of skeletal myoblasts (SkM) from limb muscle was implemented using the same culture protocol.

2.3 Differentiation induction

After serial passaging in a microsphere culture, the floating colonies of MMSCs were gently collected by centrifuge (5 mins. at 1000 rpm) or allowed to settle by gravity (20-30 mins.) and then dissociated using Cell Dissociation Solution. These dissociated cells were re-suspended and seeded on a 0.1% gelatin-coated dish in differentiation medium composed of 20ng/mL bFGF, 10ng/mL EGF, 1mM L-glutamine, 0.1mM nonessential amino acids, 2% B-27 supplement, and 10% FBS in high-glucose DMEM/Medium-199 (4:1). Growth factors including bFGF and EGF were removed from the differentiation medium as the control culture medium. Differentiation medium was refreshed every 2 days until beating cells were observed. Human recombinant growth factors were purchased from R&D Systems.

2.4 Flow cytometry or fluorescence-activated cell sorting (FACS)

Primary MMSCs cultured in Petri dishes were dissociated into single cells using non-enzymatic Cell Dissociation Solution, and then fixed in 4% paraformaldehyde for 20 mins. 1×10^5 cells were suspended in 200μl of PBS buffer containing 0.5% BSA and 2mM EDTA and incubated with the following antibodies against surface markers: c-Kit (Santa Cruz

Biotechnology), CD34 (eBioscience), CD45 (eBioscience), Flk1 (BD Biosciences), and Sca1 (Cedarlane Laboratories Ltd). Intracellular flow cytometry analysis with antibodies to Myh6 (Santa Cruz Biotechnology) and Pax-7 (Abcam) was performed after permeabilization using triton X-100 (0.1% in PBS). Unconjugated isotype antibodies were detected with FITC-conjugated donkey anti-rabbit IgG (Jackson ImmunoResearch Laboratories). After incubation with antibodies for 1 hour at room temperature, cells were washed twice with cold PBS and then re-suspended in 200μl PBS for analysis. Cell suspension was filtered through a 40μm cell strainer before sorting. Flow cytometric gates were set using control cells labeled with the appropriate isotype control antibody. Direct readout of RFP or GFP fluorescence signals was performed after cell fixation, while the same phenotypes of primary cells from wild type animals were used as control for FACS gate setting. Analyses were carried out using a BD FACSCanto II flow cytometer. The data was analyzed using computational software Modfit LT30 (Verity Software House).

2.5 Magnetic Activated Cell Sorting (MACS)

MACS Separation Kits (including microbeads) were purchased from Miltenyi Biotec (San Diego, CA). $Sca1^+$ MMSCs were sorted using MACS according to our previous publications [26, 27]. Briefly, cells were digested using Accutase (Sigma) and incubated with microbeads. Unlabeled $Sca1^-$ cells were collected by passing through the MACS column using a magnetic separator, and then the attached $Sca1^+$ cells were collected by flushing the column. The eluted fraction was then enriched by repeating the magnetic separation procedure to increase the purity of sorted cells.

2.6 Immunocytochemistry

Cardiac proteins expressed in MMSCs were identified by immunofluorescence staining. Cardiomyocytes were isolated from neonatal mice (3 days old) using a primary cell isolation kit (Thermo Fisher Scientific) as positive control. Cells cultured on slices were fixed using 4% paraformaldehyde for 20 mins. Permeabilization with 0.1% triton X-100 was added to the blocking buffer containing 1% BSA for 10 to 30 mins. The blocking process was optimized by monitoring both background and signal strength of fluorescence. After washing with PBS, antibody solution (Pax7, Nkx2-5, Isl-1, Myh6, cTnT, Myl2, or Myl7, from Abcam) was added to the slices and was incubated overnight at 4°C. After removal of the primary antibody, fluorescein-labeled secondary antibody (from Jackson ImmunoResearch) was added and incubated for 1 hour at room temperature. Nuclei were stained with DAPI, and immunostaining slices were observed with a confocal microscope (Olympus).

2.7 Electron microscope

The specimen preparation protocol for transmission electron microscopy was described in our previous publications [28, 29]. Heart tissue was isolated from adult mice (8 weeks old) as positive control. Briefly, MMSCs ($\sim 1\times10^6$) were fixed in 2% paraformaldehyde / 2.5% glutaraldehyde and then gently scraped with a cell scraper after overnight refrigeration. The resulting cell pellet was put into an Eppendorf tube and spun down at low speed. The sample was treated with 1% Osmium Tetroxide in 0.1M Cacodylate buffer for 2 hours in the refrigerator. Dehydration was performed using a graded series of ethanol (50%, 70%, 95%,

and 2×100%) and 2 × Propylene Oxide (each treatment for 15 mins.). Samples were embedded in fresh Epon resin with molds and then polymerized at 60°C in an oven overnight. Sample sectioning was performed using a diamond razor, and ultrathin sections (70 nm) were examined using an electron microscope (JEM, JEOL-USA).

2.8 Quantitative real-time PCR (qPCR)

Total RNA was isolated using Trizol reagent (Invitrogen), followed by DNAse treatment and purification using RNeasy mini column kit (Qiagen). cDNA was synthesized using miScript PCR Starter Kit (Qiagen) in a 20 μl reaction mixture. qPCR was performed on the CFX96 Real Real-time PCR system (Bio-Rad) using the miScript PCR Starter Kit protocol (Qiagen). The primers for qPCR are listed in Supplemental Table S1. All oligonucleotides used for PCR were synthesized by Eurofins Genomics (Louisville, KY). Fold changes of each target mRNA expression relative to Gapdh under experimental and control conditions were calculated based on the threshold cycle (C_T) as $r = 2^{-\Delta(\Delta C_T)}$, where $\Delta C_T = C_T(\text{target}) - C_T(\text{Gapdh})$ and $\Delta(\Delta C_T) = \Delta C_T(\text{experimental}) - \Delta C_T(\text{control})$.

2.9 Western blots

Cells were lysed with ice-cold cell lysis buffer plus protease inhibitor. Protein samples (40 μg) were mixed and resolved in 4 × SDS/PAGE sample buffer and boiled for 15 mins. before loading in 10% polyacrylamide gels (Bio-Rad). The electrophoresed proteins were transferred from the gel to PVDF membranes (Bio-Rad). Equal loading and transfer of proteins were confirmed by quantitative Ponceau red staining. The membranes were incubated for 60 mins. with 5% dry milk and Tris-buffered saline to block nonspecific binding sites of antibodies. Membranes were immunoblotted overnight at 4°C with antibodies against Nkx2-5 (Santa Cruz Biotechnology), Isl-1 (Abcam), Myh6 (Santa Cruz Biotechnology), cTnT (Abcam), or Gapdh (Sigma Aldrich) on a rocking platform. After washing with Tris-buffered saline, the membranes were incubated for 60 mins. at room temperature with HRP-conjugated secondary antibodies (Santa Cruz Biotechnology). After removal of unbound antibodies, the PVDF membranes were finally developed with an enhanced chemiluminescence plus kit (Thermo Scientific) and then exposed to X-ray film.

2.10 Measurement of calcium transients

MMSC-derived cells were dissociated by incubation with collagenase and 0.25% trypsin for 10 mins. The dissociated cells were plated onto 25-mm microscope glass coverslips coated with growth factor-free Matrigel (diluted 1:60 in RPMI medium) and cultured overnight. Cells were then incubated with 5μM Fluo-4 acetoxymethyl ester (Invitrogen) in culture medium for 2 hrs. at 37°C. Using a standard Tyrode solution, a laser-scanning confocal microscope (Olympus) was used to measure the fluorescence intensity of Fluo-4 dye from the cells on a temperature-controlled plate (37°C). Cells with Fluo-4 dye were simultaneously excited at 340 (F340) and 380 nm (F380) and emission signals were collected at 505 nm by a photomultiplier tube. Changes of Fluo-4 fluorescence intensity (indicating transient fluctuation of cytosolic calcium concentration) were recorded in frame and line-scan mode as previously described [30, 31]. Changes of intracellular Ca^{2+} content were expressed as changes in ratio ΔR = F340/F380. In addition, caffeine (Sigma) was directly added into the chamber that contained the beating MMSC-derived cells during

imaging of calcium transient. Changes of Fluo-4 fluorescence intensity were confirmed and recorded with a confocal microscope.

2.11 Whole-cell patch-clamp recordings

Patch-clamping was performed as previously described [32, 33]. MMSC-derived cells grown on coverslips were placed on the stage of the electrophysiological recording setup and perfused with a bath solution that contained 140mM NaCl, 5.4mM KCl, 1mM $MgCl_2$, 1.8mM $CaCl_2$, 5mM Na-HEPES, 0.33mM NaH_2PO_4, 10mM glucose, and 10mM HEPES (pH7.4 NaOH). For whole-cell patch-clamp recordings from a single spontaneously contracting MMSC-derived cell, electrode pipettes were made from borosilicate glass capillaries by a P-97 puller (WPI instruments) and had resistances of 3-6 MΩ when filled with internal solution. The pipette internal solution contained 140mM KCl, 1mM $MgCl_2$, 10mM HEPES, 10mM EGTA, 5mM MgATP, 10mM TEA-Cl (pH7.3 KOH). Electrophysiological signals were recorded using an Axonpatch 200B amplifier, filtered at 2 kHz, and sampled at 5 kHz using pClamp9.0 software (Molecular Device). To test membrane excitability and action potential firing, cells were recorded under current-clamp configuration. Current steps were applied to cells from −100 to 300 pA with each step at 20 pA. Step currents were injected for a duration of 2 seconds for each step and the interval between each step was 2 seconds. For measurement of I_f, cells were held at −60 mV and hyperpolarized to −140 mV for 6 seconds with each step at 10 mV, and then brought to the holding potential of −60 mV.

2.12 Measurement of cell contractile capacity

For electromechanical studies, differentiated MMSCs seeded on a 0.1% gelatin-coated glass cover-slips were analyzed for contractions in response to electrical stimulation as previously described [34]. MMSC-derived cardiomyocytes were paced with electrical field stimuli at frequencies of from 0 to 3 Hz (60 V; 25-ms square wave) using a Grass stimulator (model S88, Grass, West Warwick, RI, USA). Racemic isoproterenol (ISO, Sigma-Aldrich) was prepared fresh before each experiment. Glass coverslips containing cells were perfused with extracellular solution with or without ISO (1μM). The beating and contractile response to carbachol (1~10 μM) was also measured. Contractions were monitored and recorded digitally using a video detector (Crescent Electronics model VED-105, UT, USA) and electromechanical coupling was analyzed offline.

2.13 Statistical Analysis

Data from repeated experiments are presented as the mean ± SD. At least three independent experiments were repeated. Statistical analysis was performed using SPSS 21.0 software (IBM Corp). Data between two groups were compared using Student's T-test. Data of multiple groups were analyzed using one-way analysis of variance (ANOVA). Following ANOVA, the least significant difference post hoc test or Dunnett's t-test with Bonferroni correction were used to analyze the significance of differences between mean values of the experimental and control groups. $p<0.05$ was considered significant.

3. Results

3.1 Identification and characterization of muscle satellite cells

Satellite cells are located under the basal lamina of muscle fibers where they maintain self-renewal and regeneration potential [35]. Nkx2-5 is a mesodermal transcription factor for early SHF development [36]. The developmental origin of masseter muscle cells was determined by Nkx2-5^{Cre}/Rosa^{RFP} mice (Figure S1A). Unlike the limb skeletal muscles, masseter muscles (MM) are developed from the cardiac-PM as traced by Nkx2-5 (Figure 1A). Skeletal sarcolemma was labeled by wheat germ agglutinin (WGA), which binds to glycoproteins of the cell membrane. RFP cells were identified in the extracellular matrix (Figures 1A and S1B). Interestingly, nearly 35% of MMSCs did not express Pax7, a marker of myogenic stem cells [37] (Figure S1C). Furthermore, MMSCs were isolated from Nkx2-5^{Cre}/Rosa^{RFP} mice using a myosphere approach (Figure S1D). The freshly isolated cells were round in shape and then formed and grew into cell clusters within 5 days (Figure 1B). These cells can be expanded through serial passages as suspended myospheres for at least one month without losing proliferation capacity. A subset of the isolated cells was RFP positive, indicating expression of Nkx2-5 in their developmental history (Figure 1C). Flow cytometry (FACS) showed that about 30% of MMSCs were derived from Nkx2-5 progenitors (Figure 1D). Pax7 and stem cell antigen-1 (Sca1) were identified in MMSCs, while other progenitor markers such as c-Kit and Flk1 were not expressed. In addition, Sca1$^+$ or Sca1$^-$ cells were sorted from MMSCs to assess whether Sca1 can be used as a marker to characterize the heterogeneous phenotypes. Up to 97% of Sca1$^+$ cells can be tracked by Nkx2-5 lineage with a low level of Pax7, whereas Sca1$^-$ cells were RFP negative and highly expressed Pax7 (Figure 1 E and F). Therefore, these data indicate that Sca1$^+$ and Sca1$^-$ subsets represent two different phenotypes of MMSCs.

3.2 Comparison of differentiation potential between MMSC subsets

Osteogenic/adipogenic assay was performed to determine whether the differentiation capacity of the sorted MMSCs was distinct from mesenchymal stromal cells. Unlike Sca1$^-$ cells, Sca1$^+$ cells were not significantly induced into forming osteoblasts or adipocytes (Figure S2A). With treatment of the differentiation medium, Sca1$^-$ cells preferentially underwent myotube formation (a network of long, thin myofibers), while Sca1$^+$ cells formed flat and polygonal myocytes after spreading on culture dishes (Figure 2A). Moreover, spontaneously beating cell clusters were found in Sca1$^+$ cells (Movie S1), while irregular skeletal-like contraction was observed in Sca1$^-$ cells (Movie S2). The gene expression of MMSCs was measured by qPCR, and the limb skeletal myoblasts (SkM) were analyzed as control. The cardiogenic genes including Nkx2-5, Isl-1, Tbx5, and Gata4 were highly expressed, but the expression level of skeletal myogenic markers including MyoD, Myf5, and Pax7 was lower in Sca1$^+$ cells as compared to SkM (Figure 2B). The nuclear localization of Nkx2-5 and Isl-1 was identified in Sca1$^+$ cells (Figure 2C). Despite of expression of some cardiac progenitor markers, expression of skeletal myogenic genes in Sca1$^-$ cells was comparable to that in SkM (Figure 2B). These findings suggested that Sca1$^-$ MMSCs have prominent myogenic capacity, while Sca1$^+$ MMSCs preserve multiple cardiogenic makers.

Furthermore, we assessed whether $Sca1^+$ MMSCs possess cardiogenic potential *in vitro*. When $Sca1^+$ MMSCs were seeded and induced for up to 7 days, the expression of CM markers (including Myh6 and cTnT) was progressively upregulated, accompanied with downregulation of Nkx2-5 and Is1-1 (Figure 2D). To identify CMs permanently with a fluorescence tag, $Myh6^{Cre}/Rosa^{RFP\text{-}GFP}$ mice were generated (Figure S2B). Undifferentiated $Sca1^+$ MMSCs from these mice showed little green color and a multitude of GFP^+ cells appeared after treatment with the differentiation medium for up to 7 days (Figure 2E). FACS showed that the percentage of GFP^+ cells progressively increased during the differentiation process and reached approximately 30% at day-14 (Figure S2C). GFP was not significantly expressed in $Sca1^-$ MMSCs (Figure S2D).

3.3 $Sca1^+$ MMSCs can be converted into CM-like cells

Growth factors such as fibroblast growth factors (bFGF) and epidermal growth factor (EGF) that are important for mesoderm formation and cardiogenesis can be used to facilitate CM differentiation and growth [38, 39]. Protein levels of cTnT and Myh6 in MMSCs were significantly enhanced by the combination of B27 (serum substitute), bFGF, and EGF (Figure 3A). The expression of CM genes in MMSCs was also enhanced with the addition of these growth factors in the differentiation medium as compared to the undifferentiated cells (Figure 3B). Immunostaining of cardiac structural proteins (including cTnT and Myh6) showed that MMSCs treated with differentiation medium displayed characteristic striations indicative of sarcomere formation (Figure 3C and D) similar to neonatal cardiomyocytes. Moreover, Myl2 (ventricular isoform of myosin regulatory light chain 2) and Myl7 (atrial isoform of myosin regulatory light chain 2) were expressed in the differentiated MMSCs. Quantification of $Myh6^+$ cells showed that MMSCs were preferentially differentiated towards atrial CM-like phenotypes (Figure 3D). In addition, characteristic CM-like morphologies with organized sarcomeres and identifiable M- and Z-lines were observed in the differentiated MMSCs (Figure 3E), while adult heart tissue was used as a positive control.

The expression of Myh6 and cTnT in differentiated MMSCs decreased after Nkx2-5 siRNA treatment (Figure S3A and B). DNA methylation status and chromatin signatures of specific loci also reflect the genetic stability of lineage commitment [40]. CpG sites at the Myh6 promoter were comparatively hypermethylated in undifferentiated MMSCs, but were demethylated in differentiated cells (Figure S3C). Furthermore, the level of H3K4me3 (active promoter mark) was significantly increased at the promoter sites of the CM genes (Actn2 and Ryr2) in differentiated MMSCs, while the level of H3K27me3 (inactive promoter mark) was decreased at the cTnT promoter as compared to undifferentiated MMSCs (Figure S3D).

3.4 Induced $Sca1^+$ MMSCs display CM-like electrophysiological properties

The functionality of MMSC-derived beating cells was assessed. Basal intracellular Ca^{2+} transients were detected in differentiated MMSCs (Figure 4A). Furthermore, sarcoplasmic reticulum (SR) Ca^{2+} content was analyzed by measuring the amplitude of Ca^{2+} transients mobilized by caffeine. A rapid release of Ca^{2+} from the intracellular SR store was induced by caffeine, and the signal amplitude was increased in the induced MMSCs (Figure 4B). The

release of Ca^{2+} from the SR was linked tightly to Ca^{2+} flux through L-type Ca^{2+} channels, which is closely associated with cardiac contraction [41]. Upregulation of Ca^{2+} handling genes including Cav1.2, SERCA2a, and CSQ2 in differentiated MMSCs was also demonstrated by qPCR (Figure 4C).

The membrane excitability of MMSCs was examined by whole-cell patch-clamp recordings. The induced MMSCs spontaneously fired rebound action potentials (APs) after hyperpolarization (Figure 5A and B) and beating cells displayed APs in response to membrane depolarization. Approximately 78% of the beating cells lacked a plateau phase in their APs (Figure 5A, left panel) and were completely repolarized at about −60 mV, indicating a sinoatrial (SA) node-like AP. Moreover, 21% of the beating cells displayed a ventricular-like AP shape (Figure 5B, right panel) with a repolarization phase. AP amplitude, duration, and resting membrane potential (70.3±4.2mV) of the induced MMSCs were comparable to that seen in immature, neonatal CMs [42-44]. The β-adrenergic response of beating cells was also tested using isoproterenol (ISO). The beating rate and fractional shortening of the cells was increased by ISO stimulation (Figure 5C), but there was no impact on skeletal myotubes (Figure S4A). In addition, beating cells exhibited typical rate adaptation in response to electrical stimulation from 0.0 to 3.0 Hz (Figure 5D). Finally, spontaneous beating frequency of induced MMSCs was significantly decreased by treatment with carbachol (Figure S4B).

4. Discussion

Understanding the biological features of MMSCs provides new insight into a novel cardiac progenitor population. MM tissue may be particularly interesting as a new stem cell resource due to the accessibility, dispensability for survival, and increased muscular regeneration rate. Isolation and expansion approaches of MMSCs based on suspension culture strongly favor the processes of myogenic cell division and self-renewal [23, 45-47]. Characterization of MMSC subpopulations facilitates optimization of these approaches for manipulating stem cells. In the present study, a Sca1-labeled MMSC subpopulation was identified with a cardiogenic gene signature. Importantly, $Sca1^+$ MMSCs can be *de novo* differentiated into functional cells with CM-like morphology and electrophysiological properties.

Fate mapping studies of Isl-1 progenitors demonstrated that MM tissue and the satellite cell pool are developed from pharyngeal mesoderm [16, 48, 49]. The developmental origin of MM tissue can be demonstrated by mesodermal Nkx2-5 lineage tracing in our study. Interestingly, use of the alternative tracing model showed two different cell subsets that can be distinguished by Sca1 labeling. The isolated MMSCs are heterogeneous with respect to developmental origin, surface markers, and gene expression pattern. Heterogeneity in cell compartment contributes to the variability in cell fate and function of MMSCs. Results demonstrated that the majority of $Sca1^+$ MMSCs rather than $Sca1^-$ cells have expressed Nkx2-5 in their developmental history. Cardiac transcription factors such as Nkx2-5, Isl-1, and Gata4 were also expressed in the $Sca1^+$ MMSCs from adult mice, whereas the Pax7 expression was low. The lineage conversion of $Sca1^+$ MMSCs into CMs was demonstrated by expression of CM-specific proteins and the $Myh6^{Cre}$ reporter mice, whereas the CM transdifferentiation of $Sca1^-$ MMSCs was insufficient. Therefore, the genetic and functional

signature of Sca1$^+$ MMSCs is similar to that of embryonic cardiac progenitors, suggesting that the Sca1$^+$ MMSCs are remnants of cells from heart development. The retained expression of cardiac factors in Sca1$^+$ MMSCs indicates an epigenetic phenomenon of 'cellular memory' during development [50, 51] and the underlying mechanism(s) still requires further investigation.

Sca1$^-$ MMSCs may also originate from the cardiac-PM as shown by expression of cardiac factors such as Isl-1 and Gata4. However, this cell subtype was not developed from the mesodermal Nkx2-5$^+$ progenitors. The expression of myogenic regulatory factors such as Myf5, MyoD, and Pax7 in Sca1$^-$ MMSCs was comparable to that of limb myoblasts, consistent with the findings of unsorted jaw muscle satellite cells [48]. Additionally, Sca1$^-$ MMSCs displayed a mesenchymal stem cell phenotype as shown by the potential of osteogenesis and adipogenesis. The myogenic capacity of Sca1$^-$ MMSCs was also demonstrated by the formation of myotubes. Conversely, these characteristics were not identified in Sca1$^+$ MMSCs, indicating the functional heterogeneity of MMSCs. It is noted that this study does not exclude the existence of a minor Sca1$^-$ subpopulation with cardiogenic potential due to the variance of sensitivity for different staining and analytic techniques. The myogenic capacity of the resident Sca1$^-$ MMSC populations is important for muscle tissue homeostasis.

An evolutionary link between branchiomeric muscles and heart development in vertebrates contributes to the mechanism in which MMSCs differentiate into CMs. Cardiogenic potential was found in mouse Sca1$^+$ MMSCs in the present study. The CM-specific Myh6 and cTnT genes were only expressed in cells originating from the cranial part of the embryo (including the heart muscle), as determined by their developmental history. This finding also supports the concept of an evolutionary cardio-craniofacial field [49]. Mechanistically, distinct combinations of transcription factors such as Nkx2-5, Isl-1, and Pitx2 act upstream of skeletal myogenic or cardiogenic genes to specify different cell fates [21, 52]. The cardiogenic potential of MMSCs was blocked by Nkx2-5 knockdown, indicating the essential role of transcription factors in controlling the lineage commitment. In addition, the DNA methylation status and histone modifications at the CM genes were changed to facilitate the cardiogenic potential of MMSCs. This change of epigenetic landscape also allows for the accessibility of transcription factors to the chromatin for activation of CM genes. Therefore, CM regeneration from MMSC appears stable at the epigenetic level.

Inefficient generation of functional CMs hinders a broader application of adult stem cells. Growth factors are thought to control the early stages of mesoderm formation and cardiogenesis [38, 53]. The differentiation approach using Sca1$^+$ MMSCs was optimized using multiple growth factors. Induction with factors such as bFGF and EGF can enhance cardiac differentiation and maturation of MMSCs. Both atrial and ventricular CM-like phenotypes expressed with striated sarcomeric proteins were generated in MMSCs, although their morphology more closely resembles that of neonatal CMs rather than adult cells. Importantly, spontaneously beating cell clusters were observed in the induced MMSCs and represented a phenotype of functional CMs. The electrophysiological results suggest that the MMSC-derived beating cells had active intracellular Ca^{2+} cycling and were electrically excitable. MMSC-derived cells displayed mechanical contraction similar to neonatal CMs

and also stored large Ca^{2+} reserves in the SR for its automaticity, consistent with an earlier study [54]. Furthermore, the MMSC-derived beating cells exhibited cardiac (SA node or ventricular)-like APs. These functional characteristics of APs were similar to those observed in other cardiac-like cells derived from unsorted jaw muscle satellite cells [48]. Contraction of cardiomyocytes is modulated through β-adrenergic receptors and muscarinic acetylcholine receptors (subtype 2). Positive and negative chronotropic responses of $Sca1^{+}$ MMSC-derived beating cells were demonstrated by application of ISO and carbachol, respectively. Contraction of the derived myotubes was not impacted by ISO. These properties together indicate that the MMSC-derived cells are CM-like cells rather than a deviant phenotype of skeletal muscle. The results can further distinguish cardiogenic MMSCs from other skeletal myoblasts.

Although it is now feasible to generate CMs using cellular reprogramming techniques or by isolation of CSCs from the heart [55, 56], our study identifies an alternative progenitor source for CMs without the need for genetic manipulation or invasive heart biopsy procedures. CM generation and maturation efficiency of MMSCs in the present study remains to be enhanced robustly. The approach of purifying MMSC-derived CMs is still under development. The new CMs from MMSCs have strong potential for stem cell-based therapy, cardiac tissue engineering, or a variety of diagnostic and drug sensitivity tests. Overall, this report brings new insight into the heterogeneity of MMSCs and their developmental origin, genetic signature, and regenerative functionality.

Supplementary Material

Refer to Web version on PubMed Central for supplementary material.

Acknowledgments

This work was supported by NIH grants (HL13004201 and HL136025 to Y.W.), China National Ministry of Science and Technology key national research and development (SQ2017ZY050117; 81570279; 81370230 to P.Z.), and National Natural Science Foundation of key international cooperation research project (8171001230 to P.Z.).

References:

[1]. Yanamandala M, Zhu W, Garry DJ, Kamp TJ, Hare JM, Jun HW, Yoon YS, Bursac N, Prabhu SD, Dorn GW 2nd, Bolli R, Kitsis RN, Zhang J, Overcoming the Roadblocks to Cardiac Cell Therapy Using Tissue Engineering, J Am Coll Cardiol 70 (2017) 766–775. [PubMed: 28774384]

[2]. Oh H, Cell Therapy Trials in Congenital Heart Disease, Circ Res 120 (2017) 1353–1366. [PubMed: 28408455]

[3]. Garbern JC, Lee RT, Cardiac stem cell therapy and the promise of heart regeneration, Cell Stem Cell 12 (2013) 689–698. [PubMed: 23746978]

[4]. van Berlo JH, Kanisicak O, Maillet M, Vagnozzi RJ, Karch J, Lin SC, Middleton RC, Marban E, Molkentin JD, c-kit+ cells minimally contribute cardiomyocytes to the heart, Nature 509 (2014) 337–341. [PubMed: 24805242]

[5]. Liu Q, Yang R, Huang X, Zhang H, He L, Zhang L, Tian X, Nie Y, Hu S, Yan Y, Zhang L, Qiao Z, Wang Q-D, Lui KO, Zhou B, Genetic lineage tracing identifies in situ Kit-expressing cardiomyocytes, Cell Res 26 (2016) 119–130. [PubMed: 26634606]

[6]. Zaruba MM, Soonpaa M, Reuter S, Field LJ, Cardiomyogenic potential of C-kit(+)-expressing cells derived from neonatal and adult mouse hearts, Circulation 121 (2010) 1992–2000. [PubMed: 20421520]

[7]. Behfar A, Crespo-Diaz R, Terzic A, Gersh BJ, Cell therapy for cardiac repair-lessons from clinical trials, Nat Rev Cardiol 11 (2014) 232–246. [PubMed: 24594893]

[8]. Nigro P, Perrucci GL, Gowran A, Zanobini M, Capogrossi MC, Pompilio G, c-kit(+) cells: the tell-tale heart of cardiac regeneration?, Cell Mol Life Sci 72 (2015) 1725–1740. [PubMed: 25575564]

[9]. Nygren JM, Jovinge S, Breitbach M, Sawen P, Roll W, Hescheler J, Taneera J, Fleischmann BK, Jacobsen SE, Bone marrow-derived hematopoietic cells generate cardiomyocytes at a low frequency through cell fusion, but not transdifferentiation, Nat Med 10 (2004) 494–501. [PubMed: 15107841]

[10]. Reinecke H, Poppa V, Murry CE, Skeletal muscle stem cells do not transdifferentiate into cardiomyocytes after cardiac grafting, J Mol Cell Cardiol 34 (2002) 241–249. [PubMed: 11851363]

[11]. Wollert KC, Field LJ, Minami E, Murry CE, Reinecke H, Is There Evidence for Cardiogenic Stem Cells Outside the Heart in Adult Mammals?, Rebuilding the Infarcted Heart, CRC Press, 2007, pp. 25–40.

[12]. Abu-Issa R, Kirby ML, Heart field: from mesoderm to heart tube, Annu Rev Cell Dev Biol 23 (2007) 45–68. [PubMed: 17456019]

[13]. Wu SM, Fujiwara Y, Cibulsky SM, Clapham DE, Lien CL, Schultheiss TM, Orkin SH, Developmental origin of a bipotential myocardial and smooth muscle cell precursor in the mammalian heart, Cell 127 (2006) 1137–1150. [PubMed: 17123591]

[14]. Cai CL, Liang XQ, Shi YQ, Chu PH, Pfaff SL, Chen J, Evans S, Isl1 identifies a cardiac progenitor population that proliferates prior to differentiation and contributes a majority of cells to the heart, Dev Cell 5 (2003) 877–889. [PubMed: 14667410]

[15]. Paige SL, Plonowska K, Xu A, Wu SM, Molecular regulation of cardiomyocyte differentiation, Circ Res 116 (2015) 341–353. [PubMed: 25593278]

[16]. Harel I, Nathan E, Tirosh-Finkel L, Zigdon H, Guimaraes-Camboa N, Evans SM, Tzahor E, Distinct origins and genetic programs of head muscle satellite cells, Dev Cell 16 (2009) 822–832. [PubMed: 19531353]

[17]. Nathan E, Monovich A, Tirosh-Finkel L, Harrelson Z, Rousso T, Rinon A, Harel I, Evans SM, Tzahor E, The contribution of Islet1-expressing splanchnic mesoderm cells to distinct branchiomeric muscles reveals significant heterogeneity in head muscle development, Development 135 (2008) 647–657. [PubMed: 18184728]

[18]. Bothe I, Dietrich S, The molecular setup of the avian head mesoderm and its implication for craniofacial myogenesis, Dev Dyn 235 (2006) 2845–2860. [PubMed: 16894604]

[19]. Lescroart F, Kelly RG, Le Garrec JF, Nicolas JF, Meilhac SM, Buckingham M, Clonal analysis reveals common lineage relationships between head muscles and second heart field derivatives in the mouse embryo, Development 137 (2010) 3269–3279. [PubMed: 20823066]

[20]. Harel I, Maezawa Y, Avraham R, Rinon A, Ma HY, Cross JW, Leviatan N, Hegesh J, Roy A, Jacob-Hirsch J, Rechavi G, Carvajal J, Tole S, Kioussi C, Quaggin S, Tzahor E, Pharyngeal mesoderm regulatory network controls cardiac and head muscle morphogenesis, Proc Natl Acad Sci U S A 109 (2012) 18839–18844. [PubMed: 23112163]

[21]. Tzahor E, Heart and craniofacial muscle development: a new developmental theme of distinct myogenic fields, Dev Biol 327 (2009) 273–279. [PubMed: 19162003]

[22]. Shea KL, Xiang W, LaPorta VS, Licht JD, Keller C, Basson MA, Brack AS, Sprouty1 regulates reversible quiescence of a self-renewing adult muscle stem cell pool during regeneration, Cell Stem Cell 6 (2010) 117–129. [PubMed: 20144785]

[23]. Kuang S, Kuroda K, Le Grand F, Rudnicki MA, Asymmetric self-renewal and commitment of satellite stem cells in muscle, Cell 129 (2007) 999–1010. [PubMed: 17540178]

[24]. Murphy MM, Lawson JA, Mathew SJ, Hutcheson DA, Kardon G, Satellite cells, connective tissue fibroblasts and their interactions are crucial for muscle regeneration, Development 138 (2011) 3625–3637. [PubMed: 21828091]

[25]. Hall JK, Banks GB, Chamberlain JS, Olwin BB, Prevention of muscle aging by myofiber-associated satellite cell transplantation, Sci Transl Med 2 (2010) 57ra83.

[26]. Liang J, Huang W, Cai W, Wang L, Guo L, Paul C, Yu XY, Wang Y, Inhibition of microRNA-495 Enhances Therapeutic Angiogenesis of Human Induced Pluripotent Stem Cells, Stem Cells 35 (2017) 337–350. [PubMed: 27538588]

[27]. Kim SW, Kim HW, Huang W, Okada M, Welge JA, Wang Y, Ashraf M, Cardiac stem cells with electrical stimulation improve ischaemic heart function through regulation of connective tissue growth factor and miR-378, Cardiovasc Res 100 (2013) 241–251. [PubMed: 24067999]

[28]. Kang K, Ma R, Cai W, Huang W, Paul C, Liang J, Wang Y, Zhao T, Kim HW, Xu M, Millard RW, Wen Z, Wang Y, Exosomes Secreted from CXCR4 Overexpressing Mesenchymal Stem Cells Promote Cardioprotection via Akt Signaling Pathway following Myocardial Infarction, Stem Cells Int 2015 (2015) 659890. [PubMed: 26074976]

[29]. Chang D, Wen Z, Wang Y, Cai W, Wani M, Paul C, Okano T, Millard RW, Wang Y, Ultrastructural features of ischemic tissue following application of a bio-membrane based progenitor cardiomyocyte patch for myocardial infarction repair, PLoS One 9 (2014) e107296. [PubMed: 25310410]

[30]. Florea S, Anjak A, Cai WF, Qian J, Vafiadaki E, Figueria S, Haghighi K, Rubinstein J, Lorenz J, Kranias EG, Constitutive phosphorylation of inhibitor-1 at Ser67 and Thr75 depresses calcium cycling in cardiomyocytes and leads to remodeling upon aging, Basic Res Cardiol 107 (2012) 279. [PubMed: 22777184]

[31]. Sheikh AQ, Hurley JR, Huang W, Taghian T, Kogan A, Cho H, Wang Y, Narmoneva DA, Diabetes alters intracellular calcium transients in cardiac endothelial cells, PLoS One 7 (2012) e36840. [PubMed: 22590623]

[32]. Qian J, Vafiadaki E, Florea SM, Singh VP, Song W, Lam CK, Wang Y, Yuan Q, Pritchard TJ, Cai W, Haghighi K, Rodriguez P, Wang HS, Sanoudou D, Fan GC, Kranias EG, Small heat shock protein 20 interacts with protein phosphatase-1 and enhances sarcoplasmic reticulum calcium cycling, Circ Res 108 (2011) 1429–1438. [PubMed: 21493896]

[33]. Ikeda R, Cha M, Ling J, Jia Z, Coyle D, Gu JG, Merkel cells transduce and encode tactile stimuli to drive Abeta-afferent impulses, Cell 157 (2014) 664–675. [PubMed: 24746027]

[34]. Dai B, Huang W, Xu M, Millard RW, Gao MH, Hammond HK, Menick DR, Ashraf M, Wang Y, Reduced collagen deposition in infarcted myocardium facilitates induced pluripotent stem cell engraftment and angiomyogenesis for improvement of left ventricular function, J Am Coll Cardiol 58 (2011) 2118–2127. [PubMed: 22051336]

[35]. Montarras D, Morgan J, Collins C, Relaix F, Zaffran S, Cumano A, Partridge T, Buckingham M, Direct isolation of satellite cells for skeletal muscle regeneration, Science 309 (2005) 2064–2067. [PubMed: 16141372]

[36]. Zhang L, Nomura-Kitabayashi A, Sultana N, Cai W, Cai X, Moon AM, Cai CL, Mesodermal Nkx2.5 is necessary and sufficient for early second heart field development, Dev Biol 390 (2014) 68–79. [PubMed: 24613616]

[37]. Relaix F, Rocancourt D, Mansouri A, Buckingham M, A Pax3/Pax7-dependent population of skeletal muscle progenitor cells, Nature 435 (2005) 948–953. [PubMed: 15843801]

[38]. Schuldiner M, Yanuka O, Itskovitz-Eldor J, Melton DA, Benvenisty N, Effects of eight growth factors on the differentiation of cells derived from human embryonic stem cells, Proc Natl Acad Sci U S A 97 (2000) 11307–11312. [PubMed: 11027332]

[39]. Goldman B, Mach A, Wurzel J, Epidermal growth factor promotes a cardiomyoblastic phenotype in human fetal cardiac myocytes, Exp Cell Res 228 (1996) 237–245. [PubMed: 8912716]

[40]. Boland MJ, Nazor KL, Loring JF, Epigenetic Regulation of Pluripotency and Differentiation, Circ Res 115 (2014) 311–324. [PubMed: 24989490]

[41]. Bodi I, Mikala G, Koch SE, Akhter SA, Schwartz A, The L-type calcium channel in the heart: the beat goes on, J Clin Invest 115 (2005) 3306–3317. [PubMed: 16322774]

[42]. Nuss HB, Marban E, Electrophysiological properties of neonatal mouse cardiac myocytes in primary culture, J Physiol 479 (Pt 2) (1994) 265–279. [PubMed: 7799226]

[43]. Thomas SP, Bircher-Lehmann L, Thomas SA, Zhuang J, Saffitz JE, Kleber AG, Synthetic strands of neonatal mouse cardiac myocytes: structural and electrophysiological properties, Circ Res 87 (2000) 467–473. [PubMed: 10988238]

[44]. Yu J, Deliu E, Zhang XQ, Hoffman NE, Carter RL, Grisanti LA, Brailoiu GC, Madesh M, Cheung JY, Force T, Abood ME, Koch WJ, Tilley DG, Brailoiu E, Differential activation of cultured neonatal cardiomyocytes by plasmalemmal versus intracellular G protein-coupled receptor 55, J Biol Chem 288 (2013) 22481–22492. [PubMed: 23814062]

[45]. Poulet C, Wettwer E, Christ T, Ravens U, Skeletal muscle stem cells propagated as myospheres display electrophysiological properties modulated by culture conditions, J Mol Cell Cardiol 50 (2011) 357–366. [PubMed: 20971120]

[46]. Sarig R, Baruchi Z, Fuchs O, Nudel U, Yaffe D, Regeneration and transdifferentiation potential of muscle-derived stem cells propagated as myospheres, Stem Cells 24 (2006) 1769–1778. [PubMed: 16574751]

[47]. Tierney MT, Sacco A, Satellite Cell Heterogeneity in Skeletal Muscle Homeostasis, Trends Cell Biol 26 (2016) 434–444. [PubMed: 26948993]

[48]. Daughters RS, Keirstead SA, Slack JM, Transformation of jaw muscle satellite cells to cardiomyocytes, Differentiation 93 (2017) 58–65. [PubMed: 27918914]

[49]. Tzahor E, Evans SM, Pharyngeal mesoderm development during embryogenesis: implications for both heart and head myogenesis, Cardiovasc Res 91 (2011) 196–202. [PubMed: 21498416]

[50]. Francis NJ, Kingston RE, Mechanisms of transcriptional memory, Nat Rev Mol Cell Biol 2 (2001) 409–421. [PubMed: 11389465]

[51]. D'Urso A, Brickner JH, Mechanisms of epigenetic memory, Trends Genet 30 (2014) 230–236. [PubMed: 24780085]

[52]. Riazi AM, Lee H, Hsu C, Van Arsdell G, CSX/Nkx2.5 modulates differentiation of skeletal myoblasts and promotes differentiation into neuronal cells in vitro, J Biol Chem 280 (2005) 10716–10720. [PubMed: 15653675]

[53]. Kathiriya IS, Nora EP, Bruneau BG, Investigating the transcriptional control of cardiovascular development, Circ Res 116 (2015) 700–714. [PubMed: 25677518]

[54]. Lakatta EG, Maltsev VA, Vinogradova TM, A coupled SYSTEM of intracellular Ca2+ clocks and surface membrane voltage clocks controls the timekeeping mechanism of the heart's pacemaker, Circ Res 106 (2010) 659–673. [PubMed: 20203315]

[55]. Yoshida Y, Yamanaka S, Induced Pluripotent Stem Cells 10 Years Later: For Cardiac Applications, Circ Res 120 (2017) 1958–1968. [PubMed: 28596174]

[56]. Messina E, De Angelis L, Frati G, Morrone S, Chimenti S, Fiordaliso F, Salio M, Battaglia M, Latronico MV, Coletta M, Vivarelli E, Frati L, Cossu G, Giacomello A, Isolation and expansion of adult cardiac stem cells from human and murine heart, Circ Res 95 (2004) 911–921. [PubMed: 15472116]

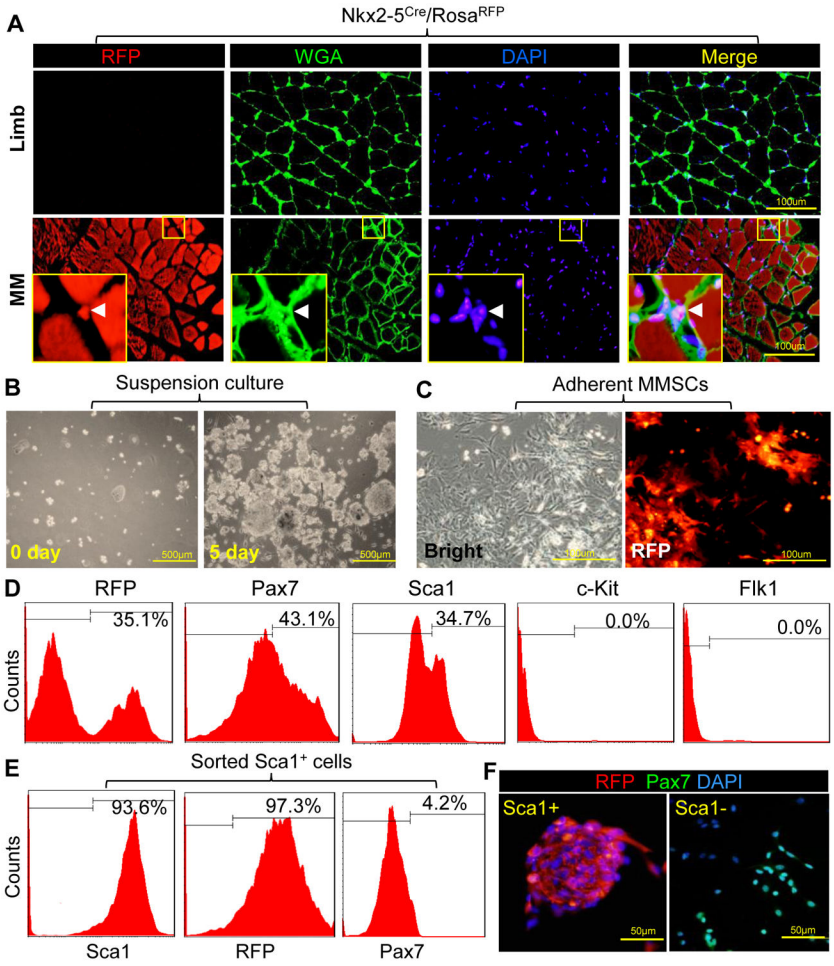

Figure 1. Identification and characterization of MMSCs.

(A): Limb or masseter muscles (MM) were isolated from Nkx2-5^{Cre}/Rosa^{RFP} mice. Tissue sections stained with wheat germ agglutinin (WGA-FITC, green) were observed under multiple channels on a confocal microscope. Arrow head in magnification view indicates the location of RFP^{+} MMSCs. (B): MMSCs were isolated and maintained in suspension culture. (C): The expression of RFP was observed by microscope after culture of MMSCs in monolayer. (D): Surface markers and RFP in MMSCs were analyzed by FACS after primary cell isolation. Flow cytometric gates (indicated by solid lines) were set using the appropriate isotype control antibody. (E): RFP and Pax7 expressions in Sca1^{+} MMSCs were analyzed by FACS after sorting. (F): Immunostaining of Pax7 and RFP expression in sorted cells was observed by microscope. Nuclei were stained with DAPI.

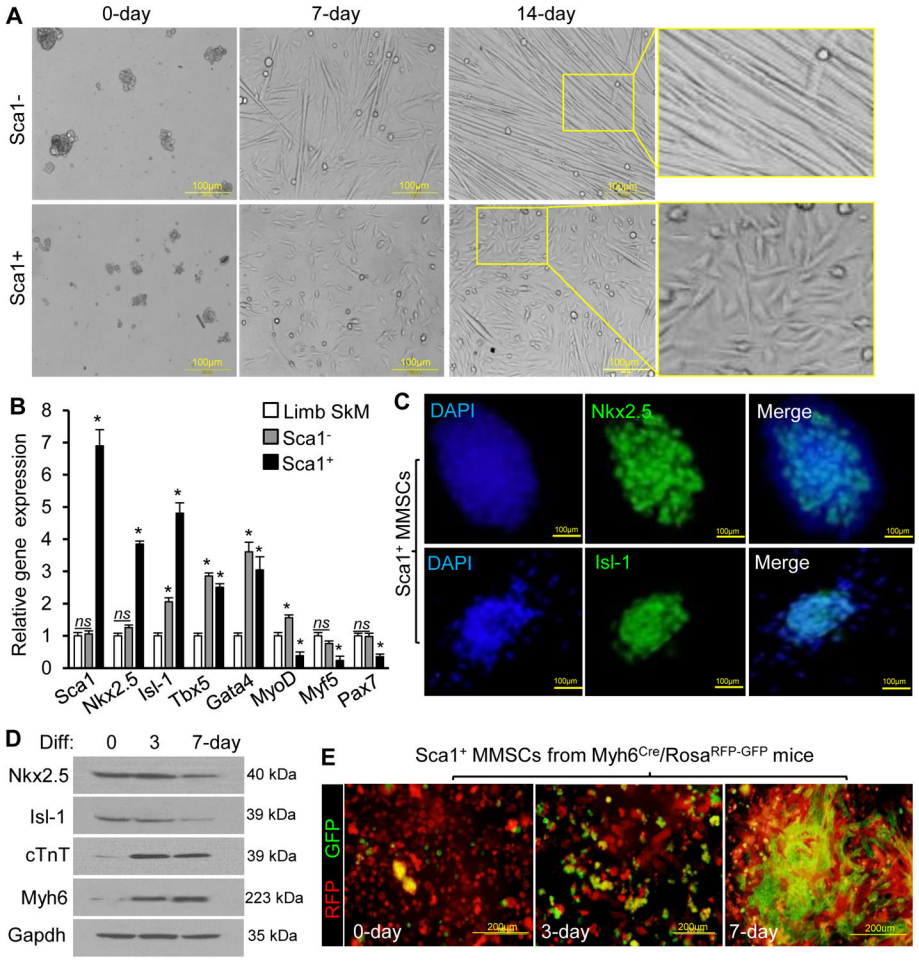

Figure 2. Cardiogenic potential of MMSCs.

(A): Representative morphologies of Sca1$^+$ or Sca1$^-$ MMSCs treated with the differentiation medium were shown under bright field microscopy. (B): Relative gene expression of cardiogenic or myogenic markers in sorted MMSCs and limb skeletal myoblasts (SkM) was analyzed by qPCR. n=4 per group. Versus SkM, * p<0.05, ^{ns} p>0.05. (C): Immunostaining of Nkx2-5 and Isl-1 in Sca1$^+$ MMSCs after cell sorting. Nuclei were stained with DAPI. (D): The protein level of cardiac progenitor or CM markers was detected by Western blotting in Sca1$^+$ MMSCs treated with differentiation (Diff.) medium. Identical results were observed in 3 independent experiments, each with technical triplicates. (E): The expression of RFP and GFP in Sca1$^+$ MMSCs from transgenic mice was observed by microscope after differentiation.

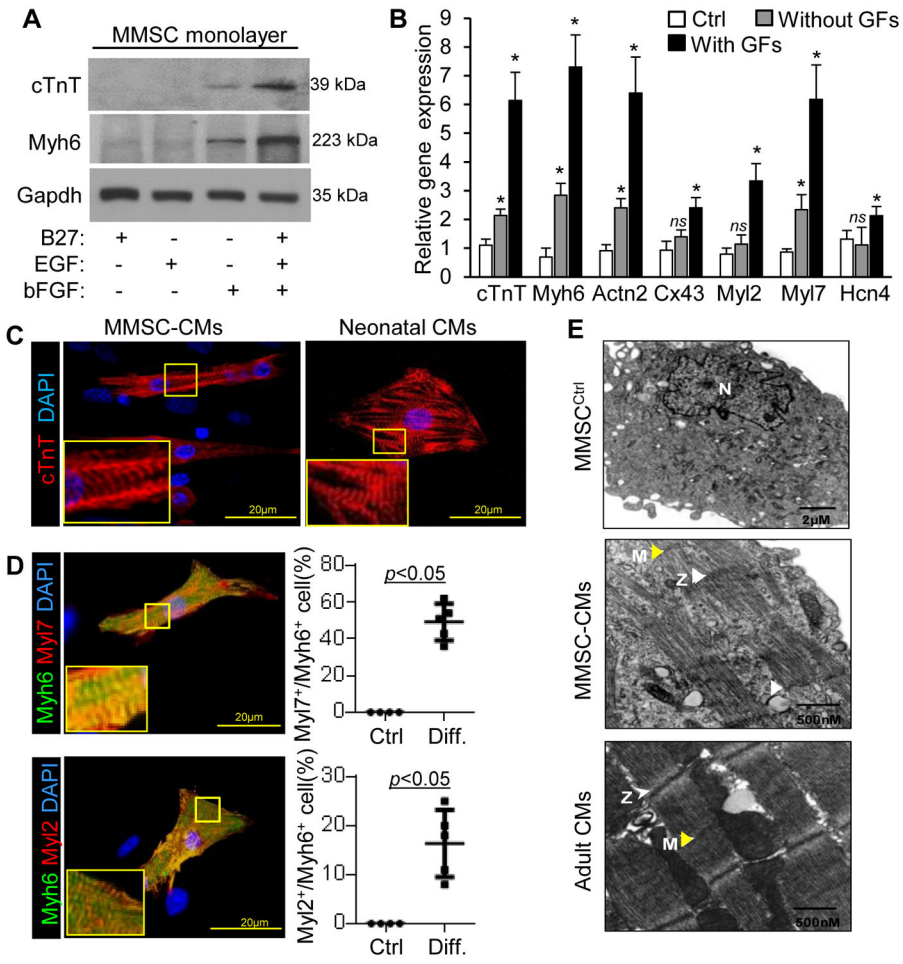

Figure 3. Phenotypes of Sca1$^+$ MMSC-derived cells.

(A): Myh6 and cTnT were analyzed by Western blotting in MMSCs treated with various growth factors. Identical results were observed in 3 independent experiments, each with technical triplicates. (B): The relative expression of CM markers in undifferentiated MMSCs (Ctrl) or MMSCs treated with or without growth factors (GF) including bFGF and EGF was analyzed by qPCR. n=4 per group. Versus Ctrl, * p<0.05, ^{ns} p>0.05. (C): CM markers were analyzed by immunostaining in MMSCs after induced with growth factors. The percentage of Myl2$^+$ or Mly7$^+$ cells in undifferentiated (Ctrl, n=4) or differentiated (Diff. n=5) MMSCs was showed. (D): Representative transmission electron imaging of undifferentiated (Ctrl) or differentiated MMSCs. Yellow and white arrows show M- and Z-lines respectively.

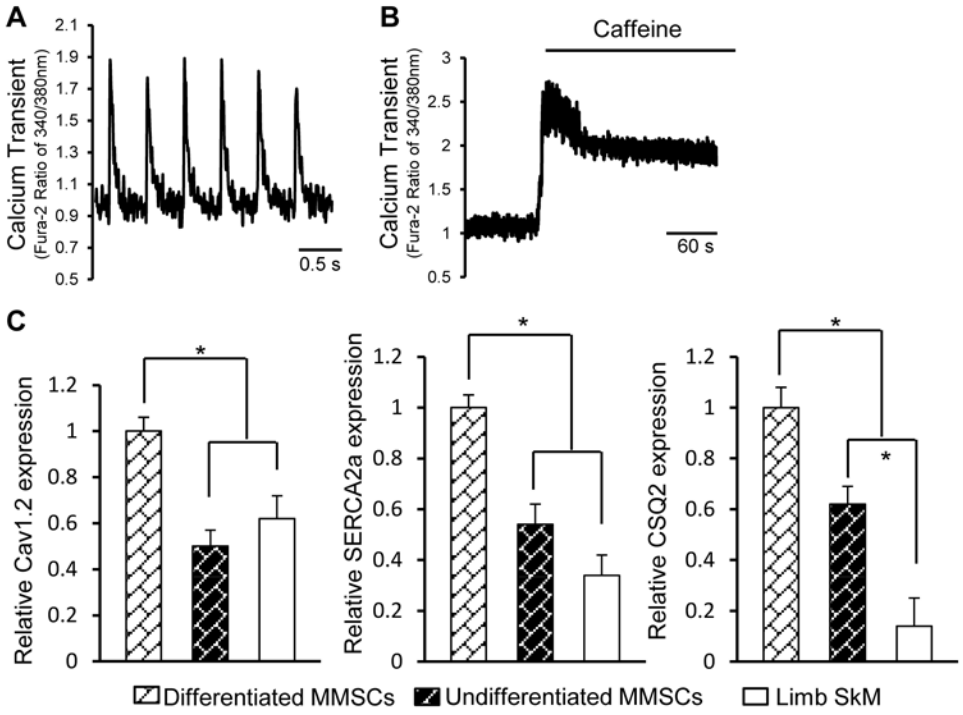

Figure 4. Electrophysiological properties of Sca1^{+} MMSC-derived cells.

(A): Measurement of Ca^{2+} transient frequency in MMSC-derived beating cells loaded with Fura-2 fluorescent dye. (B): Ca^{2+} transient of MMSC-derived cells in response to caffeine (5mM). (C): Calcium handling gene expression in differentiated MMSCs, undifferentiated MMSCs, and limb skeletal myoblasts (SkM) was analyzed by qPCR. n=5 for each group; *p<0.05.

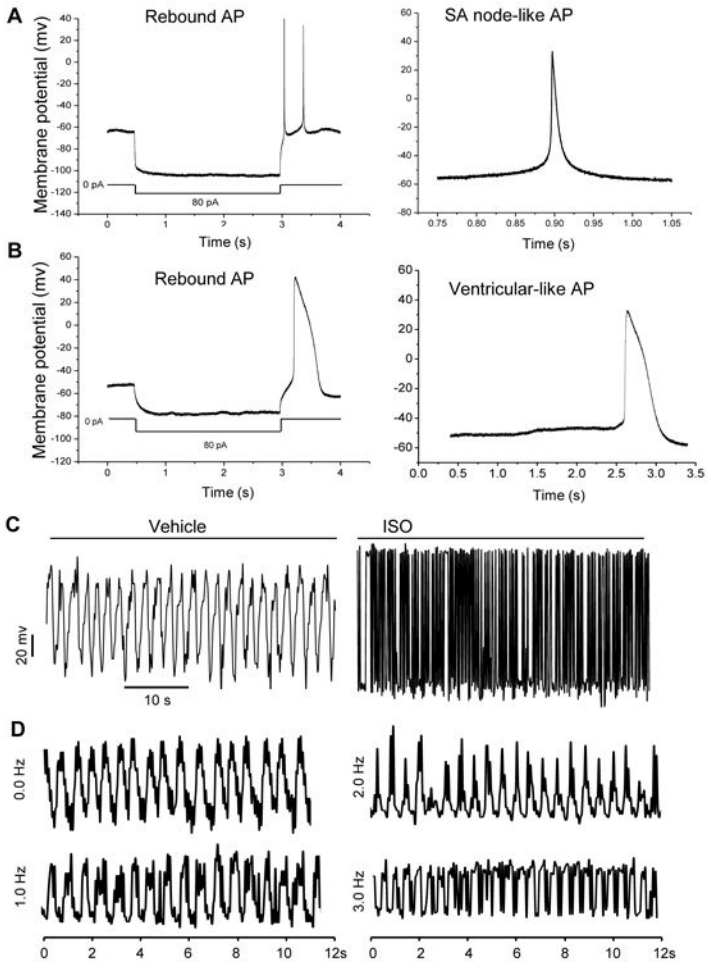

Figure 5. Electrophysiological properties of MMSC-derived cells.

(A and B): Action potentials (APs) of the MMSC-derived beating cells were measured by whole-cell patch-clamp recording. Rebound APs of MMSC-derived beating cells after hyperpolarization. Identical results were observed in 3 independent experiments, each with technical triplicates. (C): Contractility analysis of CM-like cells treated with or without β-adrenergic receptor agonist ISO (1μM). (D): Mechanical response of MMSC-derived myocytes to electrical stimulation. Frequencies of electrical stimulation from 0.0 to 3.0 Hz were measured by using video edge detection.